Sensitized Red Luminescence from Bi^{3+} co-doped Eu^{3+} : $ZnO\text{-}B_2O_3$ Glasses

Atul D. Sontakke, Anal Tarafder, Kaushik Biswas and K. Annapurna*[1]
Glass Technology Laboratory, Central Glass and Ceramic Research Institute
(Council of Scientific and Industrial Research)
196, Raja S.C. Mullick Road, Kolkata- 700032, India.

Abstract

Photoluminescence properties of Bi^{3+} co-doped Eu^{3+} containing zinc borate glasses have been investigated and the results are reported here. Bright red emission due to a dominant electric dipole transition $^5D_0 \rightarrow {}^7F_2$ of the Eu^{3+} ions has been observed from these glasses. The nature of Stark components from the measured fluorescence transitions of Eu^{3+} ions reveal that the rare earth ions could take the lattice sites of C_s or lower point symmetry in the zinc borate glass hosts. The significant enhancement of Eu^{3+} emission intensity by 346 nm excitation ($^1S_0 \rightarrow {}^3P_1$ of Bi^{3+} ions) elucidates the sensitization effect of co-dopant. The energy transfer mechanism between sensitizer (Bi^{3+}) and activator (Eu^{3+}) ions has been explained.

Keywords: Zinc borate glasses; Bi^{3+} sensitization; Eu^{3+} emission; energy transfer

PACS: 32.50.+d, 33.50.-j, 42.70.-a, 42.70.Ce.

* Corresponding author: Tel.: +91-33 2473 3469; Fax: +91-33 2473 0957
Email: glasslab42@hotmail.com (K. Annapurna), annapurnak@cgcri.res.in

1. Introduction

The spectroscopic properties of Eu^{3+} ion have extensively been investigated in different host materials due to its intense *red* emission [1-3]. Many Eu^{3+}-doped materials are of commercial importance in the display devices as efficient *red* emitting phosphors [4-6] and solid-state lasers [7]. The Eu^{3+} ions are also being used as a probe ion to study the local crystal field effect of host materials because of the forced electric dipole transition $^5D_0 \rightarrow {}^7F_2$, which is hypersensitive to relatively smaller changes in the chemical surroundings of the luminescent active ion [8].

In recent years, heavy metal oxides such as bismuth (Bi), lead (Pb) and tellurium (Te) based glasses have attracted more attention because of their low phonon energies, extended infrared transmission and high non-linear optical properties which are applicable in non-linear optoelectronics including optical fiber and optical switches. Bismuth in glasses plays a dual role as a glass network former (NWF) at high concentration and a modifier (NWM) at low concentration. In addition to this, Bi^{3+} ions possess interesting luminescence characteristics in the high-energy region ranging from UV-Vis and also in the low-energy IR region of the electromagnetic spectrum. The materials showing IR emission of Bi^{3+} ions in the wavelength range 1000-1400 nm depending upon the excitation energy have drawn much consideration by many research groups because they can cover first communication window [9]. The current efforts in the development of mercury-free fluorescence lamp and plasma display panels (PDP) need the phosphors, which are having significant absorption or excitation in the VUV region and emission in the visible. For PDP and display applications, rare earth doped

compounds are usually employed as phosphor materials. An enhancement in the luminescence efficiency of rare earth doped materials have been observed on co-doping with Bi^{3+} ions because of their strong absorption bands in the VUV-UV region and capability of energy transfer to active ions suggesting the role of Bi^{3+} ions as a sensitizer to the rare earth ions [10, 11]. The position of Bi^{3+} absorption and emission bands strongly depend on host materials due to large expansion of *s* and *p* orbitals of Bi^{3+} ions, which ultimately influence the energy transfer efficiency of Bi^{3+} ions [12]. Thus, the sensitization effect of Bi^{3+} on active ions varies from host to host. Among the glassy hosts, zinc borate glasses possess some uniqueness in effectively absorbing UV region and transferring it to the active ions, which enables them for potential industrial applications in the forms of Solar blind UV sensor and optical fiber with a large core diameter etc. Earlier in the literature, an efficient fluorescence has been reported from Eu^{3+} and Tb^{3+} doped zinc borate glasses under an UV excitation due to an energy transfer from direct band gap ZnO crystallites present in those glasses [13].

Hence, in the present work, the sensitization effects of the Bi^{3+} ions on the luminescence properties of Eu^{3+} ions in $60ZnO\text{-}40B_2O_3$ glasses has been systematically investigated as a function of Bi^{3+} concentration.

2. Experimental

The glasses with the chemical composition in mol% of $60ZnO\text{-}(40\text{-}x)B_2O_3\text{-}0.2Eu_2O_3\text{-}xBi_2O_3$ (x = 0, 0.1, 0.2, 0.5, 1.0) were prepared by a conventional melt quenching method. Appropriately weighed and thoroughly mixed batches of reagent grade oxide chemicals were sintered at 300°C for 12 h and were melted in platinum

crucible at 1100°C for 45 min with an intermittent stirring to obtain homogeneous melt. Each of the melts was poured at 1000°C on preheated graphite mold followed by annealing at 450°C for 1 h and slowly cooling to the room temperature. The obtained glasses were cut and polished for their analysis purpose. The glass samples have been labeled as Bi0-Bi1.0 depending upon the Bi_2O_3 concentration for convenience.

The densities of the glasses were measured by Archimedes' method using water as immersion liquid. Refractive indices ($n_{F'}$, n_e and $n_{C'}$) of the glasses were obtained on a Pulfrich refractometer (Model: PR 2) at three different wavelengths of 480nm, 546.1nm and 643.8nm respectively. The optical absorption spectra of all (Eu^{3+}, Bi^{3+})-codoped zinc borate glasses were recorded on a Perkin-Elmer Lambda-20 spectrophotometer in the wavelength range of 200–600 nm. Both emission and excitation spectra were measured on a Spex Fluorolog-2 Spectrofluorimeter equipped with a 150 W Xe - lamp as an excitation source.

3. Results and Discussion

3.1 Physical and optical properties

Some of the important physical and optical properties of zinc borate glasses doped with 0.2 mol% $Eu_2O_3$and varied contents of Bi_2O_3 from 0 to 1.0 mol% are presented in Table 1. It is clear from this table that, the average molecular weight (M_{avg}) and density (d) of the glasses are found to be increasing with the Bi^{3+} addition, which may be due to the inclusion of heavy metal ions (Bi^{3+}) in the glass matrix. The density related other physical parameters such as Molar volume (V_M), Eu^{3+} ion concentration (N_{Eu}), Interionic

distance (r_i), Polaron radius (r_p) and Field strength (F) of all zinc borate glasses have also been computed using the relevant formulae [14, 15]. Normally, when the density (d) of the material increases, its molar volume (V_M) decreases, but the present zinc borate glass series have shown a linear dependence of molar volume with their density variation i.e., both density and molar volume increased indicating the opening up of glass network which may be due to the formation of non-bridging oxygen (NBOs) with the inclusion of Bi^{3+} ions. The measured refractive indices of the glasses at three different wavelengths have been used to evaluate the optical properties such as Abbe number (ν_e), Reflection loss (R%), Molar refractivity (R_M), and non linear optical properties of the glasses such as nonlinear refractive index (n_2), nonlinear coefficient (γ) and third order nonlinear susceptibility ($\chi_{1111}^{(3)}$) [16-18]. The obtained data are presented in the same table. The refractive indices of these glasses show the similar trend as density, increasing linearly with the Bi_2O_3 content, which can be attributed to the hyper-polarizability of the Bi^{3+} ions possessing $6s^2$ lone pairs in its valence orbital. Due to this, it can be seen from the Table 1 that the overall non-linear properties of the glasses have been increased.

3.2 Spectral Analysis

3.2.1 Absorption Spectra

Fig. 1 shows the room temperature absorption spectra of (Bi^{3+}, Eu^{3+})-codoped zinc borate glasses. The spectra reveal the absorption bands of Eu^{3+} ion due to transitions from its ground state multiplets such as $^7F_0$ and thermally populated $^7F_1$ levels to the upper levels of $4f^6$ configuration. As in the case of Eu^{3+} ions, the ground state $^7F_0$ and the higher-level $^7F_1$ are very close to each other (around 380 cm^{-1}) so that at room

temperature a significant amount of $^7F_1$ levels are thermally populated [19, 20]. This results in a characteristic absorption spectrum of Eu^{3+} ions exhibiting closely spaced doublets. In the present study, the recorded absorption peaks for all glasses are assigned to the corresponding transitions of $^7F_0 \rightarrow {}^5D_0$, $^5D_1$, $^5D_2$, $^5D_3$, $^5L_6$, $^5G_3$, $^5G_4$, $^5D_4$ and $^7F_1 \rightarrow {}^5D_0$, $^5D_1$, $^5L_6$, $^5D_4$ respectively depending upon their peak energies. It is observed from this figure that, the overall absorbance of the glasses has been found to be slightly increasing with an increase in Bi_2O_3 content. This may be attributed to a small increase in reflection losses (R%) at their surfaces due to enhancement of refractive indices with the increase of bismuth content. Another interesting observation made from the absorption spectra of these glasses is that, the UV band edge is found to be shifting towards a lower energy with an increase of Bi_2O_3 content in the glasses. This red shift in the UV cut-off wavelength with the change of Bi_2O_3 content indicates a strong absorption due to Bi^{3+} ions, which lies in the UV region [21, 22].

3.2.2 Emission and Excitation Spectra

The measured photoluminescence spectra of (Bi^{3+}, Eu^{3+})-codoped zinc borate glasses with an excitation at 392 nm ($^7F_0 \rightarrow {}^5L_6$ of Eu^{3+}) have uniformly exhibited emissions from both $^5D_1$ and $^5D_0$ excited levels to the ground state multiplets of Eu^{3+} ions. The Fig. 2 presents a specimen profile of emission spectrum of Eu^{3+}-doped zinc borate glass. Among the emission bands detected, the five bands in the wavelength range of 570-750 nm centered at 580 nm, 594 nm, 615 nm, 655 nm and 708 nm are due the transitions $^5D_0 \rightarrow {}^7F_{0,\,1,\,2,\,3\,\&\,4}$ and two weak emissions in the wavelength range 520-560 nm at 528 nm and 555 nm are assigned to the transitions of $^5D_1 \rightarrow {}^7F_{1\,\&\,2}$ respectively.

Relatively low intensities of emissions from $^5D_1$ are attributed to the presence of high energy phonons (around 1300 cm^{-1}) in the borate glass, which enables a faster decay of the $^5D_1$ excited level to the lower lying $^5D_0$ level resulting in a dominant luminescence from $^5D_0$ excited level to the ground state multiplets. Because of the fact that the emissions from $^5D_0$ to ^7F_J of Eu^{3+} ion could play an important role as probe in understanding the local field symmetry, the recorded fluorescence spectrum in Fig. 2 has been analyzed critically and following important facts have been made. The emission due to $^5D_0 \rightarrow {}^7F_0$ transition at 582 nm is normally forbidden, however in the present host, it is observed in moderate emission intensity. Two strong emission bands centered at 594 nm ($^5D_0 \rightarrow {}^7F_1$) and 615 nm ($^5D_0 \rightarrow {}^7F_2$) could be attributed to the magnetic dipole (MD) and forced electric dipole (ED) transitions respectively. The forced electric dipole transition appears when Eu^{3+} ions occupy non-inversion lattice centers, whereas the magnetic dipole transition appears due to inversion center lattices [23-24]. Therefore, the ratio between integrated intensities of these two transitions ($I_{5D0 \rightarrow 7F2}/I_{5D0 \rightarrow 7F1}$) directly elucidates the asymmetry nature around Eu^{3+} ions in the host. In the present glass system its value is found to be 2.982. Such a large value of the asymmetric ratio and the existence $^5D_0 \rightarrow {}^7F_0$ transition with a moderate intensity substantiates the presence of strong crystal field (CF) in the vicinity of rare earth ion causing Stark splitting in electric dipole ($^5D_0 \rightarrow {}^7F_2$) and magnetic dipole ($^5D_0 \rightarrow {}^7F_1$) transitions. In spite of the site-to-site difference which prevails in amorphous materials; the later transition shows clearly three Stark components while the former at 615 nm has exhibited five components from the deconvolution as shown in the inset of Fig. 2. Based on the selection rules, the observed number of three and five Stark components for magnetic and electric dipole transitions of

Eu^{3+} ions respectively could reveal the fact that, the dopant rare earth ions take C_s or lower symmetry sites in the present glass network [25].

By monitoring the prominent red emission of Eu^{3+} ($^5D_0 \rightarrow {}^7F_2$) at 615 nm the excitation spectra of (Eu^{3+}, Bi^{3+})-codoped zinc borate glasses have been recorded and shown in Fig. 3. The different excitation peaks at 317 nm, 360 nm, 381 nm, 392 nm, 412 nm, 462 nm and 524 nm are assigned to the transitions $^7F_0 \rightarrow {}^5H_6$, $^5D_4$, ^5G_j, $^5L_6$, $^5D_3$, $^5D_2$, $^5D_1$ and peaks at 398 nm and 530 nm are due to the transitions from thermally populated $^7F_1$ level to the $^5D_1$ and $^5L_6$ excited levels of Eu^{3+} ions respectively. These observations are fully in agreement with the measured absorption spectra as described in the earlier section. Further, it is clear from Fig. 3 that, the excitation spectra have also demonstrated variation in the UV region with the change in the Bi_2O_3 concentration. The excitation peak at 317nm due to transition $^7F_0 \rightarrow {}^5H_6$ of Eu^{3+} ions is found to be disappearing with the formation of a broad band at around 329 nm upon the introduction of bismuth in the glass. This band shows a gradual shift towards the longer wavelength (346 nm) with the increasing Bi_2O_3 concentration and is attributed to electronic transitions of Bi^{3+} ions. The Bi^{3+} ion with $6s^2$ electronic configuration possesses the ground state $^1S_0$ and four excited states $^3P_0$, $^3P_1$, $^3P_2$ and $^1P_1$ in the order of increasing energy. The transitions between the ground state $^1S_0$ and ^3P_j excited levels are spin-forbidden; however the $^1S_0 \rightarrow {}^3P_1$ transition becomes partially allowed by mixing with the singlet state and triplet state of Bi^{3+} ions. The observance of Bi^{3+} absorption bands strongly depends on the host matrix. In several hosts, two absorption bands have been reported, which belong to the transitions of $^1S_0 \rightarrow {}^3P_1$ and $^1P_1$ [22, 27]. The later band lies in the high energy UV region than the

former one which appears at relatively lower energy. In certain hosts, a single absorption band has been observed at longer wavelength (~ 320 nm) due to the $^1S_0 \rightarrow {}^3P_1$ transition [12, 23, 26]. The absence of the $^1P_1$ absorption band could be due to its possible overlapping with the fundamental absorption region of the host. The $^1S_0 \rightarrow {}^3P_1$ absorption transition of Bi^{3+} ion is usually located at wavelength around 300 nm and is strongly influenced by the covalency of Bi^{3+} bonding, which varies with the nature of the surrounding ligands. If the electronegativity of the ligand decreases, the absorption band shifts towards a longer wavelength [27]. Hence, from the present (Eu^{3+}, Bi^{3+})-codoped zinc borate glass system, the observed excitation band which is found between 329 nm and 346 nm depending upon the Bi^{3+} ion concentration belongs to the $^1S_0 \rightarrow {}^3P_1$ transition of Bi^{3+} ion. The detection of this excitation band due to Bi^{3+} by monitoring Eu^{3+} emission indicates an influence of Bi^{3+} on Eu^{3+} fluorescence.

In order to examine the effect of Bi^{3+} codoping on the emission of Eu^{3+} ions, the fluorescence spectra of Eu^{3+} doped and (Eu^{3+}, Bi^{3+})-codoped zinc borate glasses under the excitation of Bi^{3+} ions into $^3P_1$ level have been measured and is shown in Fig. 4. It is clear from this figure that, even the Eu^{3+}-doped glass without Bi^{3+} revealed Eu^{3+} emission from $^5D_0$ to $^7F_{0,\ 1,\ 2,\ 3,\ 4}$ ground state multiplets, this may be due to the non-resonant excitation into the closely packed upper laying levels of Eu^{3+} which later cascades down to $^5D_0$ level. Upon the inclusion of Bi^{3+} ions in the glass, the intensity of these transitions has been significantly enhanced. In addition to this, a broad emission band peaking at 484 nm has been observed with a gradual increase in its intensity with an increase in Bi^{3+} concentration. This band is assigned to the Bi^{3+} emission due to $^3P_1 \rightarrow {}^1S_0$ transition.

Thus the Stokes shift between excitation ($^1S_0 \rightarrow {}^3P_1$) and emission ($^3P_1 \rightarrow {}^1S_0$) of Bi^{3+} ions is found to be around 8240 cm^{-1}, which demonstrates an extension of the energy level of Bi^{3+} ions in this host. With the concentration of Bi_2O_3 range from 0.1 mol% to 1.0 mol% keeping the Eu^{3+} concentration constant at 0.2 mol% in zinc borate glasses, a two folds increase in the Eu^{3+} intensity has been observed. This enhancement in the Eu^{3+} intensity on inclusion of the Bi^{3+} ions indicates the energy transfer between Eu^{3+} and Bi^{3+} ions in the present zinc borate glasses. The energy transfer mechanism in this system has been understood by studying excitation spectra systematically.

The energy transfer among sensitizer and activator is mainly due to a radiative transfer through emission of sensitizers and re-absorption by activators or/and non-radiative transfer associated with the resonance condition between the sensitizer and the activator ions. The efficiency of the radiative energy transfer depends on how competently the activator ions are excited by the emission of sensitizers. It requires a significant overlap of the emission of the sensitizer and the absorption of the activator. The non-radiative energy transfer is accompanied by the electric multipole interactions and exchange interactions. However, the probability of total energy transfer is proportional to the energy overlap between the emission of sensitizers and absorption of activators, whether the transfer has been caused by a radiative decay, exchange or multipole interactions. Thus the energy overlap plays a crucial role in the energy transfer from sensitizers to activators [28-29]. Fig. 5 shows the emission and excitation spectra of Bi^{3+} and Eu^{3+} doped zinc borate glasses respectively. It can be seen that the emission band of Bi^{3+} ions overlaps appreciably on the excitation peaks of $^5D_1$, $^5D_2$ and $^5D_3$ of Eu^{3+}

ions satisfying the condition for an energy transfer. Hence, it is obvious to attribute the enhancement of Eu^{3+} emission intensity in the zinc borate glasses codoped with Bi^{3+} ions to the energy transfer from Bi^{3+} to Eu^{3+} ions.

In an effort to further confirm and understand the energy transfer mechanism in this system, the excitation spectra of (Eu^{3+}, Bi^{3+})-codoped zinc borate glasses have been measured by monitoring $^5D_1 \rightarrow {}^7F_1$ transition at 528 nm as this level is totally overlapping on the emission band of Bi^{3+} ions. Fig. 6 shows the excitation spectra of (Eu^{3+}, Bi^{3+})-codoped zinc borate glasses monitoring the Eu^{3+} emission at 528 nm. From this figure it is clear that, the spectra revealed only two excitation peaks; one is a strong broad band in the range of 329-346 nm and the other is relatively narrow at 392 nm. The first peak has been assigned to $^3P_1 \rightarrow {}^1S_0$ transition of Bi^{3+} and the later one to $^7F_0 \rightarrow {}^5L_6$ transition of Eu^{3+}. The relative intensity ratio of these two peaks has been observed to be varying from 0.54 to 1.93 for Bi0.1 to Bi1.0 glasses respectively, signifying the contribution of Bi^{3+} excitation to the $^5D_1$ level emission of Eu^{3+} is increasing with the increase of bismuth concentration over the $^5L_6$ level excitation of Eu^{3+} ions. Thus, the strong Bi^{3+} excitation band for the Eu^{3+} emission indicates an efficient energy transfer from Bi^{3+} to Eu^{3+} in this host glass. The possible energy transfer mechanism has been explained with the help of an energy level diagram of Bi^{3+} and Eu^{3+} ions as in inset of Fig. 5. However, it is to mention here that the energy transfer from Bi^{3+} to Eu^{3+} is not full but only a partial. This is established with the co-existence of Bi^{3+} emission band in the fluorescence spectra as depicted in Fig. 4.

Also it is observed from Fig. 4 that, the emission intensity of Eu^{3+} increases rapidly at lower concentration of Bi_2O_3 showing more than two fold enhancements for Bi0.5 glass (0.5 mol% of Bi_2O_3). The inset of Fig. 4 shows the relationship between emission intensity of Eu^{3+} ions with the Bi_2O_3 concentration in the zinc borate glasses. For small Bi_2O_3 concentration, the Eu^{3+} intensity increases rapidly, however it shows saturation at higher Bi_2O_3 concentrations. It is obvious that the sensitized effectiveness of the Bi^{3+} ions on the Eu^{3+} emission varies with the Bi^{3+} concentration, which indicates the difference in the probability of energy transfer from Bi^{3+} ions to Eu^{3+} ions. The observed saturation in the increase of Eu^{3+} emission intensity at higher concentration of Bi^{3+} could be explained as follows. In a sensitizer-activator doped system, the energy transfer efficiency depends not only on the probability of energy transfer from sensitizer to activator but also on the activator to sensitizer back transfer and/or on the probability of energy transfer amongst the sensitizers [28]. In order to examine any occurrence of energy back transfer, the excitation spectra of (Bi^{3+}, Eu^{3+})-codoped glasses have been recorded by monitoring the Bi^{3+} emission at 484 nm as shown in Fig. 7. The spectra exhibit only a single band due to Bi^{3+} ions; thus it is clear to that there is no back transfer of energy from Eu^{3+} to Bi^{3+} ions in the zinc borate glass system.

When the probability of an energy transfer amongst the sensitizers increases, an excitation of sensitizers could often be followed by either one or several sensitizers before a sensitizer to the activator energy transfer could occur. These transfers are often accompanied by a small amount of energy of absorption due to relaxation of lattice and quenching sites. It is therefore quite evident that, energy transfer between sensitizers will

reduce the probability of energy transfer to activators. Thus, at high Bi^{3+} concentration, the Eu^{3+} emission intensity tends to saturate because of the reduction in the probability of energy transfer from Bi^{3+} to Eu^{3+} accompanied by an increase in Bi^{3+} ion emission.

4. Conclusions

The sensitization effectiveness of the Bi^{3+} ions on the luminescence properties of Eu^{3+} ions in the zinc borate glasses has been investigated as a function of Bi^{3+} concentration. The Eu^{3+} ions are found to occupy the lattice sites of C_s or lower point symmetry in the present zinc borate glasses. A single excitation band due to $^1S_0 \rightarrow {}^3P_1$ transition of Bi^{3+} ions has been observed which is found to be shifting towards the longer wavelength with an increase in Bi^{3+} content in the glasses resulting in a broad structure less emission located at 484 nm due to $^3P_1 \rightarrow {}^1S_0$ transition. The emission intensity of Eu^{3+} ions has been enhanced by more than two folds with the Bi^{3+} addition in the glasses. This enhancement in the luminescence properties of Eu^{3+} ions is attributed to an efficient energy transfer from Bi^{3+} to Eu^{3+} ions in this host. For lower concentration of Bi^{3+} ions in the glass, intensity enhancement is observed to be rapid, showing a maximum enhancement for the glass with 0.5 mol% Bi_2O_3, while any further increase of Bi^{3+} concentration showed saturation due to an increase of probability of energy migration among Bi^{3+} ions.

Acknowledgements

Authors would like to thank Dr. H. S. Maiti, Director, CGCRI for his kind encouragement and permission to publish this work. Our thanks are also due to Dr. Ranjan Sen, for his kind support in the present work. One of us (Mr.ADS) is thankful to the CGCRI, CSIR for the award of Research Internship to him.

References

[1] J. S. Bae, J. H. Juong, Song-Soo Yi and Jung-Chul Park, Appl. Phys. Lett. 82 (2003) 3629.

[2] Wang Xiao-Xiao, Jing Wang, Shi Jian-Xin, Qiang Su, Gong Meng-Lian, Mater. Res. Bull. 42 (2007) 1669.

[3] X. Zhao, X. Wang, B. Chen, Q. Meng, W. Di, G. Ren, Y. Yang, J. Alloys and Compd. 433 (2007) 352.

[4] H. M. Yang, J. X. Shi, M. L. Gong, J. Solid State Chem. 178 (2005) 917.

[5] R. P. Rao, D. J. Devine, J. Lumin. 87-89 (2000) 1260.

[6] A. Poloman, J. Appl. Phys. 82 (1997) 1.

[7] W. M. Krupke, USPTO 20060153261 (2006).

[8] E. W. J. L. Oomen, A. M. A. van Dongen, J. Non-Cryst. Solids 111 (1989) 205.

[9] Y. Arai, T. Suzuki, Y. Ohishi, S. Morimoto, S. Khonthon, Appl. Phys. Lett. 90 (2007) 261110.

[10] W. J. Park, S.G. Yoon, D. H. Yoon, J. Electroceram. 17 (2006) 41.

[11] C. Gao, L.Chen, J. Bao, Y. Fu, G. Zhang, J. Electrochem. Soc. 154 (2007) J345.

[12] C. H. Kim, H.L. Park, S. Mho, Solid State Commun. 101 (1997) 109.

[13] D. Ruter, W. Bauhofer, Appl. Phys. Lett. 69 (1996) 892.

[14] M. M. Ahmad, E. A. Hogarth and M. N. Khan, J. Mater. Sci. 19 (1984) 4041.

[15] A.J. Glass laser program annual report, Lawrence-Livermore Labs. Report No. URCL-50021-72 (1975).

[16] M. J. Weber, J. E. Lynch, D. H. Blackburn and D.T. Cronin, IEEE J. Quantum Electron, 19 (1983) 1600.

[17] S. H. Kim, J. Yoko and S. Sakka, J. Am. Ceram. Soc. 76 (1993) 865.

[18] H. E. Rast, J. C. Fry and H. H. Casper, J. Chem. Phys., 46 (1967) 1460.

[19] W. T. Carnall, P. R. Fields, K. Rajnak, J. Chem. Phys. 49 (1968) 4450.

[20] A. Ivankov, J. Seekamp, W. Bauhofer, J. Lumin.121 (2006) 123.

[21] M. J. Weber, R. R. Monchamp, J. Appl. Phys. 44 (1973) 5495.

[22] C. Lei, J. Yang, Z. Guo-Bin, W. Can, Y. Guang-Tao, W. Chun, L. Guo-Hua, Chin. Phys. Lett. 25 (2008) 1884.

[23] J. Yang, L. Yang, W. Liu, Y. Zhang, H. Fan, Y. Wang, H. Liu, J. Lang, D. Wang, J. Alloys and Compd. 454 (2008) 506.

[24] M. Bettinelli, A. Speghini, M. Ferrari, M. Montana, J. Non-Cryst. Solids 201 (1996) 211.

[25] Fuxi Gan, "Laser Materials", World Scientific Pub. Pte. Ltd., Singapore 1995.

[26] Y. Porter-Chapman, E. Bourett-Courchesne, S.E. Derenzo, J. Lumin. 128 (2008) 87.

[27] X. Zeng, S. Im, S. Jang, Y. Kim, H. Park, S. Son, H. Hatanaka, G. Kim, S. Kim, J. Lumin. 121 (2006) 1.

[28] M. Wang, X. Fan, G. Xiong, J. Phys. Chem. Solids 56 (1995) 859.

[29] G. Blasse, A. Bril, J. Electrochem. Soc. 115 (1968) 1067.

Figure Captions

Fig. 1: Absorption spectra of (Eu^{3+}, Bi^{3+})-codoped zinc borate glasses.

Fig. 2: Fluorescence spectrum Eu^{3+}-doped zinc borate glass. (Inset: Deconvolution of $^5D_0 \rightarrow {}^7F_2$ transition)

Fig. 3: Excitation spectra of (Eu^{3+}, Bi^{3+})-codoped zinc borate glasses.

Fig. 4: Emission spectra of (Eu^{3+}, Bi^{3+})-codoped zinc borate glasses under Bi^{3+} excitation (inset: Variation of red emission of Eu^{3+} as a function of Bi_2O_3 content)

Fig. 5: Energy overlap between (a) excitation of Eu^{3+} and (b) emission of Bi^{3+} in (Eu^{3+}, Bi^{3+})-codoped zinc borate glasses.

Fig. 6: Excitation spectra of (Eu^{3+}, Bi^{3+})-codoped zinc borate glasses.

Fig. 7: Excitation spectra of (Eu^{3+}, Bi^{3+})-codoped zinc borate glasses.

Table 1: Physical and optical properties of (Eu^{3+}, Bi^{3+})-co doped zinc borate glasses.

Properties	Bi0	Bi0.1	Bi0.2	Bi0.5	Bi1.0
Physical					
M_{avg} (g/mol)	77.24	77.64	78.04	79.23	81.21
d (g/cm^3)	3.701	3.723	3.745	3.786	3.866
V_M (cm^3)	20.87	20.85	20.84	20.93	21.01
N_{Eu} (10^{20} ion/cm^3)	1.154	1.155	1.156	1.151	1.147
r_i (Å)	20.54	20.53	20.53	20.56	20.58
r_p (Å)	8.28	8.27	8.27	8.28	8.29
F (10^{14} cm^2)	4.38	4.38	4.38	4.37	4.36
Optical					
n_e (546.1nm)	1.6709	1.6716	1.6761	1.6816	1.6911
$n_{F'}$ (480.0nm)	1.6781	1.6789	1.6835	1.6891	1.6991
$n_{C'}$ (643.8nm)	1.6642	1.6648	1.6692	1.6742	1.6836
($n_{F'}$ - $n_{C'}$)	0.0139	0.0141	0.0143	0.0149	0.0155
ν_e	48.28	47.68	47.15	45.74	44.51
R%	6.31	6.32	6.38	6.46	6.59
R_M	2.60	2.60	2.58	2.57	2.55
n_2 (10^{-13} esu)	2.73	2.79	2.87	3.04	3.25
γ (10^{-16} cm^2/W)	0.68	0.70	0.72	0.76	0.81
$\chi_{1111}^{(3)}$(10^{-14} esu)	1.11	1.14	1.17	1.25	1.34

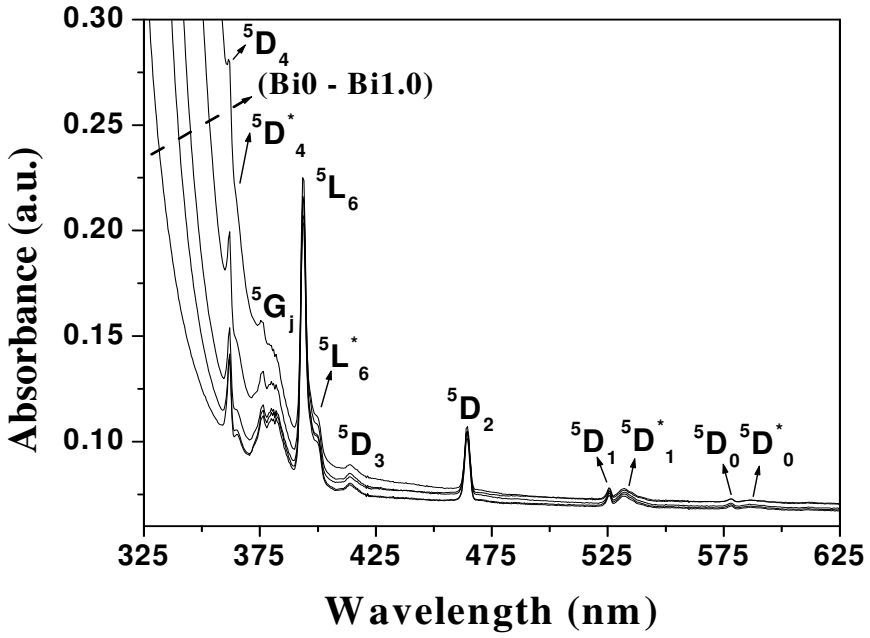
0.30
0.25
0.20
0.15
0.10
Absorbance (a.u.)
325
375
425
475
525
575
625
Wavelength (nm)
$^5D_4$
(Bi0 - Bi1.0)
$^5D^*_4$
$^5L_6$
^5G_j
$^5L^*_6$
$^5D_3$
$^5D_2$
$^5D_1$
$^5D^*_1$
$^5D_0$
$^5D^*_0$

Fig. 1

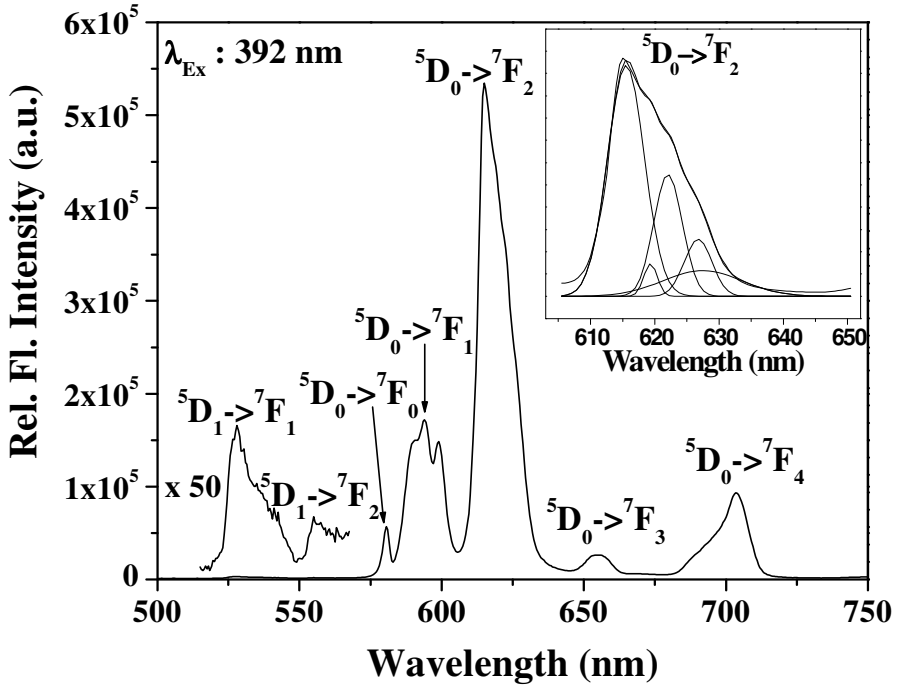
λEx : 392 nm
5D0->7F2
5D0->7F1
5D0->7F0
5D1->7F1
5D1->7F2
5D0->7F3
5D0->7F4
x 50
Rel. Fl. Intensity (a.u.)
Wavelength (nm)
6x10^5
5x10^5
4x10^5
3x10^5
2x10^5
1x10^5
0
500
550
600
650
700
750
5D0->7F2
610
620
630
640
650
Wavelength (nm)

Fig. 2

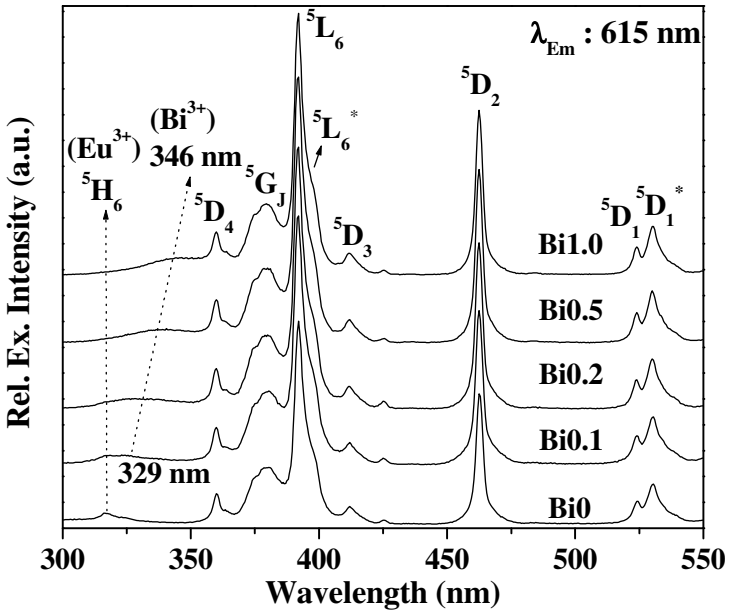
Rel. Ex. Intensity (a.u.)
Wavelength (nm)
300
350
400
450
500
550
λ_{Em} : 615 nm
$^5L_6$
$^5D_2$
$^5L_6{}^*$
(Bi^{3+})
346 nm
(Eu^{3+})
$^5H_6$
$^5D_4$
^5G_J
$^5D_3$
$^5D_1$
$^5D_1{}^*$
Bi1.0
Bi0.5
Bi0.2
Bi0.1
Bi0
329 nm

Fig. 3

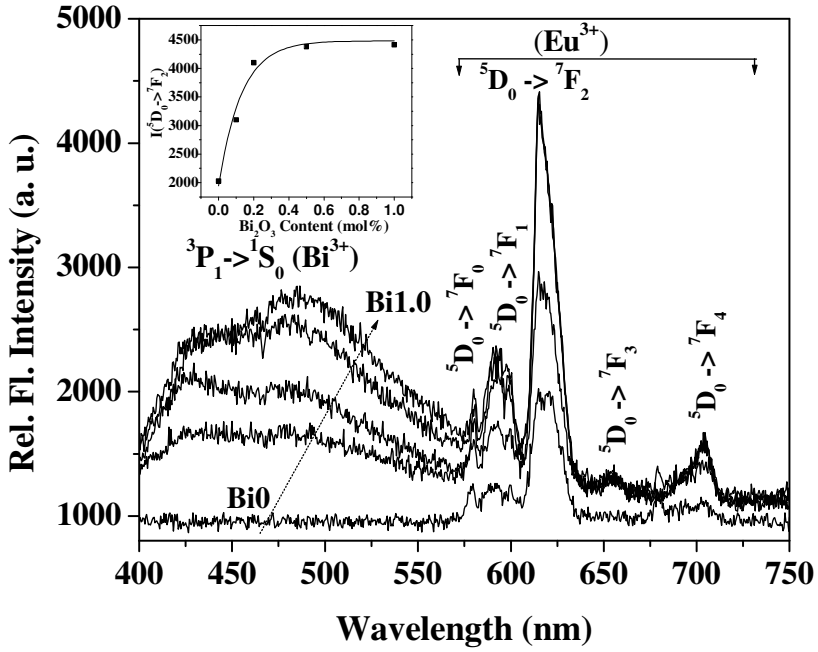
Rel. Fl. Intensity (a. u.)
Wavelength (nm)
(Eu3+)
5D0 -> 7F2
3P1->1S0 (Bi3+)
Bi1.0
Bi0
5D0 -> 7F0
5D0 -> 7F1
5D0 -> 7F3
5D0 -> 7F4
I(5D0->7F2)
Bi2O3 Content (mol%)

Fig. 4

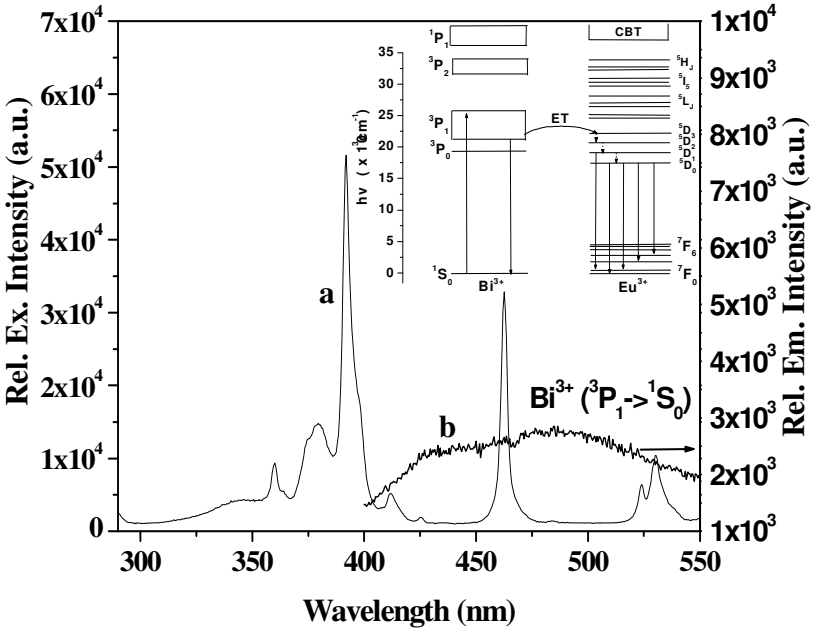
Rel. Ex. Intensity (a.u.)
Rel. Em. Intensity (a.u.)
Wavelength (nm)
a
b
Bi3+ (3P1->1S0)
CBT
ET
1P1
3P2
3P1
3P0
1S0
Bi3+
Eu3+
7F6
7F0

Fig. 5

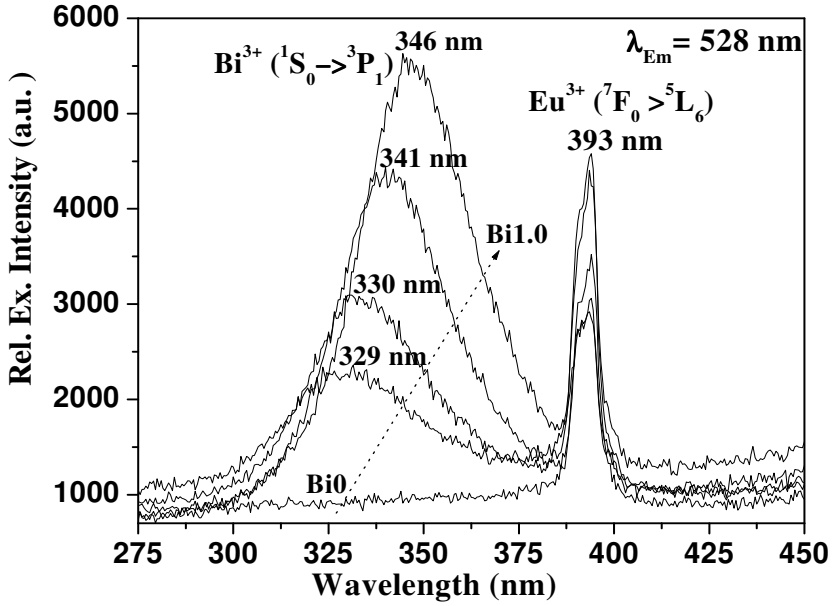
Rel. Ex. Intensity (a.u.)
Wavelength (nm)
λEm = 528 nm
Bi3+ (1S0 -> 3P1)
346 nm
341 nm
330 nm
329 nm
Bi1.0
Bi0
Eu3+ (7F0 > 5L6)
393 nm
6000
5000
4000
3000
2000
1000
275
300
325
350
375
400
425
450

Fig. 6

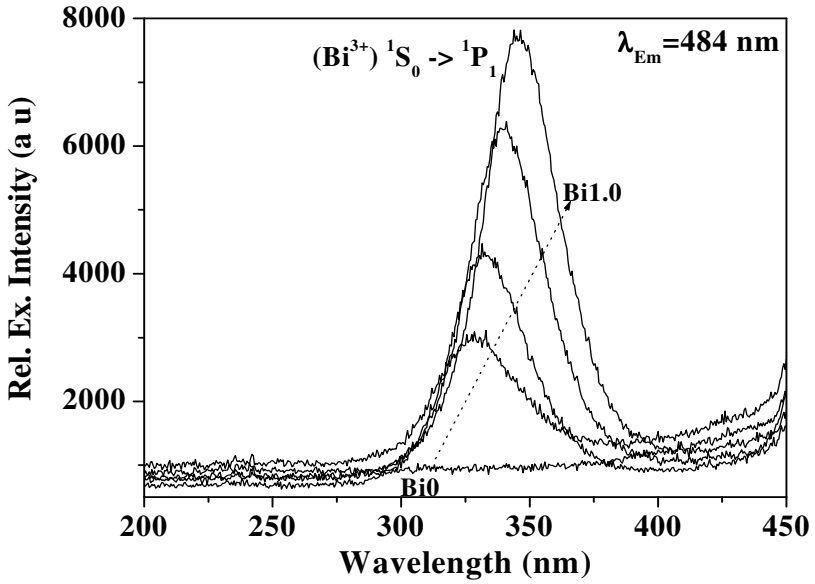
8000
6000
4000
2000
Rel. Ex. Intensity (a u)
200
250
300
350
400
450
Wavelength (nm)
(Bi3+) 1S0 -> 1P1
λEm=484 nm
Bi1.0
Bi0

Fig. 7